Journal of Sound and Vibration (1997) **206**(5), 697–724

EXTREME-VALUE PREDICTION FOR NON-LINEAR STOCHASTIC OSCILLATORS VIA NUMERICAL SOLUTIONS OF THE STATIONARY FPK EQUATION

J. F. Dunne and M. Ghanbari

School of Engineering, The University of Sussex, Falmer, Brighton, BN1 9QT, England

(*Received* 26 *September* 1996, *and in final form* 4 *June* 1997)

The accuracy of two well-established numerical methods is demonstrated, and the importance of "bandwidth" examined, for computationally efficient Markov based extreme-value predictions associated with finite duration stationary sample paths of a non-linear oscillator driven by Gaussian white noise. By making the Poisson assumption of independent upcrossings, extreme exceedance probabilities are predicted via the mean threshold crossing rate, using numerical solutions of the stationary Fokker–Planck (FPK) equation. With bandwidth initially ignored, predicted exceedances using the Weighted Residual methods of Bhandari and Sherrer, Soize, and Kunert, and the Finite Element method of Langley, are compared with nominally "exact" predictions for a heavily damped Duffing-type model obtained by using an explicit FPK solution—the FE method being established as superior. Predictions via FE solutions are then compared with very long Monte Carlo simulations, in which bandwidth effects are included. Two lightly damped non-linear oscillator models are examined, both with cubic stiffness, but different damping mechanisms—one model again being of simple Duffing-type with linear damping, the other being appropriate to single co-ordinate random vibration of a clamped–clamped beam, with wholly non-linear damping. The realistic damping parameter values assigned to the beam model are statistically equivalent to the linear damping level chosen for the simple model, at just above 1%. At this overall damping level, results clearly demonstrate that, for the probability levels and durations considered, bandwidth is only important for the linearly damped model—for the beam model with non-linear damping, bandwidth can be ignored, allowing accurate extreme exceedance predictions by using only the stationary FPK equation. The paper also demonstrates that the "limiting decay rate of the first-passage probability"—advocated by Crandall, Roberts and others, as a criterion for deciding the barrier height above which first-passage times can be assumed independent—proves grossly over-conservative as a corresponding criterion for deciding the independence level for use in stationary extreme-value prediction.

1. INTRODUCTION

Reliability assessment of dynamically sensitive structures with stochastic loading can be assisted by using two wholly complementary statistical approaches: (i) via the "reliability" function or first-passage probability, or (ii) via extreme-value analysis [1]. Much important work has been done over the past three decades on theoretical first-passage prediction for use with oscillator models in structural reliability assessment [1, 2–7], but the theoretical base for extreme-value prediction is much less complete. Extreme-value statistics are important because they give useful information about the maximum value of key response variables within a specified period of time, in a form which can also be compared directly with the risk of other extreme events occurring elsewhere. There is currently a need for accurate and efficient prediction of low exceedance probabilities, from the tails of the

0022–460X/97/400697 + 28 $25.00/0/sv971148

extreme-value distribution function associated with realistic oscillator models of random vibration, by using methods which can be embedded unobtrusively within a more general structural reliability procedure. The stochastic type loading mentioned here arises, for example, in mathematical models of offshore structures exposed to ocean waves, buildings undergoing seismic disturbances, wind buffeting or turbulence problems on aircraft or bridges, and in rolling contact problems on irregular surfaces. When it is assumed that particular difficulties in physical modelling and parameter assignment can be overcome, the two most serious problems which can arise in the use of these models stem either from strong non-linearity in system behaviour or from sources of excitation which cannot adequately be modelled as stationary normal processes. The occurrence of either problem generally prevents confident use of linear dynamic analysis with extreme-value theory for normal processes [8, 9]. Here the focus of attention is on the first type of problem, namely prediction of extreme-value statistics for a non-linear oscillator excited by a stationary normal stochastic process.

The task of obtaining exact extreme-value distribution functions for short duration sample paths of a general stochastic process, remains an unsolved problem [10]. In one important approximate approach via asymptotic theory [8], it is assumed, for practical purposes, that the extreme-value distribution function has converged within a finite time interval, to one of three specific types (I, II, or III). In using these asymptotic models it is first necessary to establish the distribution type, and then to estimate unique values of the distribution scale and location parameters—these are available in closed form only for normal processes [8]. For non-normal responses, the only practical way to obtain these parameters for non-linear oscillator models is via simulated data. But even when using selective estimation methods, which offer significant efficiency gains over conventional approaches [11], confident prediction of low extreme exceedance probabilities still requires a large extreme-value sample size. To meet this requirement very long Monte Carlo simulations are needed, but these often prove unacceptable in practice. There have been many methods developed to obtain reasonably good approximations to various non-linear oscillator response statistics [12, 13], although in the specific role of extreme-value prediction, the accuracy of these methods is largely unknown, except for the standard method of statistical linearization, which is known to be severely in error for strongly non-linear behaviour. Some specific extreme-value prediction methods have been developed by using a combination of theory, simulation and extrapolation [1, 14–17]. Winterstein and Ness [14] for example, developed a general two-stage method via Hermite moment closure and analytical model fitting (which can also be used with limited simulations or measured data [16] if complete knowledge of a dynamic model is lacking). Predictions of (i) Morison-type fluid forces on cylinders; and (ii) responses of Duffing and hysteretic oscillator models, give accurate (median) extreme-values, fatigue damage estimates, and crossing rates. For more complex non-linear oscillator models however, high-order moment closure is required, significantly increasing the complexity of the method. Naess *et al*. [15] used extended linearization for strongly non-linear systems via an alternative to the usual minimum mean square error criterion. Accurate extreme exceedance probabilities were obtained for simple Duffing models, and for oscillators with linear stiffness and quadratic damping. Obvious potential exists for use of this method on MDOF systems, but the error criterion depends critically on the extreme level and the type of non-linearity. The first author, Dunne [17], used optimal control theory, plus short simulations, to obtain highly accurate extreme local maxima exceedance probabilities for oscillators with strongly non-linear stiffness and damping, driven by narrow-band Gaussian excitation. Corresponding extreme-value statistics can also be obtained, but the method cannot be used where conventional local maxima theory proves sensitive or fails

totally (e.g., for an oscillator driven by unlimited bandwidth white noise). Clearly there is still a need for a direct, accurate, and efficient approach to extreme-value prediction, for realistically non-linear oscillator models driven by white noise excitation, which does not involve complicated intermediate stages, system dependent non-linearities, or simulation.

One direct theoretical route to the extreme value distribution function via threshold crossing statistics uses only the mean upcrossing rate [18]. This asymptotic approach is justified when the Poisson assumption of independent up-crossings holds: i.e., for relatively high thresholds and long durations. To obtain stationary crossing statistics, only the joint probability density function for the response and its first derivative is needed. But for lower thresholds or short time durations, the effect of "bandwidth" may demand modification to the Poisson assumption [1, 8] ("bandwidth" is taken to mean the concentration of energy on response sample paths within a narrow-band of frequencies, an effect which usually means successive local maxima are highly correlated). The effort needed to make this modification however, even when practically possible, goes well beyond the requirements of crossing statistics alone and therefore, in particular applications, strong evidence is needed to justify it. Conversely, if bandwidth is not important, the threshold crossing approach is attractively simple.

By contrast, if exact first-passage probabilities are obtained, a similar independence assumption is not required at non-extreme levels, even though such predictions may prove computationally very expensive. There are however good physical reasons for assuming first-passage intervals also become independent above certain finite "barrier" heights [3, 7], opening up the possibility of very efficient approximate predictions based on the Poisson assumption. Indeed the so called "limiting decay rate of the first-passage probability" has been studied by several researchers [2–7], as a criterion for deciding the (first-passage) barrier height above which the Poisson assumption holds for linear and non-linear oscillator responses. It is not known in general however, whether this same criterion extends equally well to stationary extreme-value prediction. Therefore in focusing attention on the accuracy of efficient extreme-value prediction via threshold crossing statistics, the suitability of the limiting decay-rate criterion needs to be demonstrated.

Now, for a general class of non-linear oscillator models, the mean threshold crossing rate can be obtained via Markov process theory by using the stationary Fokker–Planck–Kolmogorov (FPK) equation [19]. Although many numerical solution methods have been developed, very little is known about their accuracy in extreme-value prediction. Moreover stationary FPK solutions contain no information about the structure of a stochastic process at the sample level, and are therefore insufficient to account for the effects of bandwidth. This deficiency would seemingly limit the use of the stationary FPK equation as an approach to extreme response statistics. But those examples cited so far demonstrating the importance of bandwidth (see, e.g., reference [1]) have been justifiably restricted to very simple oscillator models with light linear damping. This raises the question whether the effect of bandwidth is actually significant for extreme-value prediction associated with a realistic system with non-linear damping.

In this paper, initially (in section 2), a synopsis is given of a very large number of well established methods which might be used to solve the stationary FPK equation. The accuracy of two methods in particular (the WRM and the FEM) are then tested specifically to obtain efficient FPK based extreme-value exceedance probabilities, namely by comparison with nominally "exact" predictions for a simple Duffing oscillator. Three different shape functions are tested in the WRM and just one in the FEM. This test is designed to find an acceptable numerical FPK solution method (rather than to exhaust the relative merits of each) in order to establish—for two lightly damped non-linear

oscillators with statistically equivalent damping levels—the importance of bandwidth in extreme-value prediction, and second, to demonstrate the accuracy of a highly efficient prediction method based only on the stationary FPK equation.

2. A SYNOPSIS OF NUMERICAL METHODS FOR SOLVING THE FPK AND BK EQUATIONS

Since a large number of numerical FPK solution methods have been developed over the past 30 years, it is appropriate before making use of two of them to explain briefly the main uses of both FPK and BK equations in structural dynamics, and to give a brief qualitative overview of specific methods. Also particular articles will be identified which give good reviews to these specific methods, so this synopsis will justify the choice of the methods tested in section 4 and subsequently used in section 5.

The (forward) Fokker–Planck (FPK) equation and its closely related adjoint: the Backward Kolmogorov (BK) equation, are parabolic time-dependent partial differential equations used to describe transition probabilities associated with continuous state Markov processes in N dimensions (equation (10) of this paper is an FPK equation). Full descriptions of these equations as applied in structural dynamics can be found in references [13, 19, 20] where they are mainly used in obtaining response moments, density functions, crossing- or first-passage statistics. First-passage probabilities for example, which have played such a prominent role in failure studies, can be approached via the ''reliability'' function—either by solving a BK-type, or Forward FPK equation—whereas first-passage moments can be obtained directly from the simpler Pontryagin–Vitt equation [13]. Initial conditions can be modelled as deterministic or as ''random start'' with specified distribution. Various types of (partially open) boundary condition can be used to model different types of first-passage failure. For example, a ''B''-type barrier imposes a single-sided absorbing boundary, a ''D''-type models a double barrier, and more complicated contour barriers are also possible such as the (circular) ''C''-type. The use of different barriers can have a significant influence on the probability of first-passage failure [3–5]. When the FPK boundaries are closed, or the barrier level is allowed to move to infinity, stationary solutions are possible if the normalization condition (which imposes no loss of probability) is satisfied for all time. Stationary solutions can be used, for example, to obtain various low-level response statistics and higher-order information such as the mean crossing rate. And from a computational viewpoint stationary solutions can either be obtained with an eigenfunction expansion of a non-stationary FPK equation (using the eigenvector associated with a zero eigenvalue [7]), or directly from a stationary FPK (by imposing time independence [19]). In the first-passage problem the normalization condition is only satisfied initially, so the FPK/BK solution is never stationary. However, under appropriate conditions a limit state is reached known as ''the limiting decay rate of the first-passage probability'' [2–7]. This decay rate is equal to the smallest eigenvalue in an eigenfunction expansion of a non-stationary FPK or BK equation with appropriate boundary conditions—(reference [6] details many different numerical methods which have been designed to obtain approximate first-passage statistics via the limiting decay rate, by using the ''decay-rate over mean-crossing-rate'' ratio as a criterion to justify the approach). As shall be seen shortly, the FPK equation has not been used to any extent in extreme-value analysis.

In discussing particular numerical approaches one distinguishes here between two types of approximation: (i) those methods which are intended to give specific insight and reasonably good approximations to FPK or BK equations (or a suitably reduced version),

and (ii) "numerical" methods, which, if fully utilized, should in practice be able to approach the exact solution with virtually negligible error (these methods are shown in Table 1). Type (i) methods will not be discussed here (which include for example Van Kampen expansions, stochastic averaging, moment methods and others, which, along with known explicit solutions, are covered in references [13, 20]), even though an examination of the literature over the past 30 years, shows that the number of publications using type (i) methods considerably outstrips the number using any one of our (five) specific "numerical" categories.

Table 1 gives a sample of users of type (ii) numerical methods. This list is not definitive since there are many non-structural applications omitted, for example in physics and biology (particularly astro-, plasma-, particle- and chemical physics). Within the five categories listed, contributors have variously obtained stationary or non-stationary solutions of 1D, 2D or 3D problems.

TABLE 1

Some contributors to the development and use of numerical methods for solving the forward FPK and backward Kolmogorov equations

Method	Contributors
Weighted residuals	R. G. Bhandari and R. E. Sherrer (1968) [21] C. Soize (1989) [22] A. Kunert (1991) [23]
Finite element	L. A. Bergman and J. C. Heinrich (1981) [24] L. A. Bergman and B. F. Spencer Jr (1983) (see ref. list [26]) R. S. Langley (1985) [25] L. A. Bergman (1989) (see ref. list [26]) H. P. Langtangen (1991) (see ref. list [26]) B. F. Spencer Jr and L. A. Bergman (1993) [26] H. T. Banks, H. T. Tran and D. E. Woodward (1993) [27] H. U. Köylüoglu, S. R. K. Nielsen and R. Iwankiewicz (1994) [28] M. A. Elgebeily and H. E. E. Shabaik (1994) [29]
Path integration (cell mapping)	M. F. Wehner and W. G. Wolfer (1983) (see ref. list [32]) T. Kapitaniak (1985) [30] J.-Q. Sun and C. S. Hsu (1988) [31] J.-Q. Sun and C. S. Hsu (1990) (see ref. list [32]) A. Naess and J. M. Johnsen (1991) [32] A. Naess and J. M. Johnsen (1991) (see ref. list [32]) A. N. Drozdov (1992) [33] H. U. Köylüoglu, S. R. K. Nielsen and R. Iwankiewicz (1995) (see ref. list [34]) H. U. Köylüoglu, S. R. K. Nielsen and A. C. Cakmak (1995) [34] R. Iwankiewicz and S. R. K. Nielsen (1996) [35]
Finite difference	J. B. Roberts (1986) [5] J. S. McKenzie, M. R. O'Brian and M. Cox (1991) [36] E. M. Epperlein (1994) [37] B. T. Park and V. Petrosian (1996) [38] W. V. Wedig (1996) [39]
Variational method —Eigenfunction expansion	T. K. Caughey (1971) (see ref. list [7]) J. D. Atkinson (1973) (see ref. list [7]) J. P. Johnson and R. A. Scott (1980) (see ref. list [7]) M. Yar and J. K. Hammond (1986) (see ref. list [7]) R. S. Langley (1988) [7]

The earliest approach shown is the weighted residual method (WRM) [21–23] which is typically used to solve a stationary or non-stationary FPK equation via weighted orthogonal functions and Galerkin's method. (Reference [22] gives perhaps the most detailed application of this method.)

Closely related to the WRM is the Finite Element method (FEM) which uses simple piece-wise orthogonal shape functions defined over finite, rather than an infinite region, thus allowing greater flexibility in satisfying complicated boundary conditions. Application of the FEM has been fully described in a series of more than 16 publications, starting around 1981 with that of Bergman and Heinrich, [24] (addressing numerical first-passage prediction by using a Petrov–Galerkin solution of the BK equation), through to the more recent use of the (simpler) Bubnov–Galerkin solution of the FPK by Spencer and Bergman [26]. Reference [26] actually gives a thorough review of FEM developments up to 1993. Langley [25] independently developed an efficient stationary FEM in which finite elements were also used to approximate drift terms in the FPK equation. It should be mentioned that some specific problems known to occur with the FEM (and finite differences) include for example when the drift terms dominate diffusion. Banks *et al*. [27], combined the FEM with the method of characteristics to avoid erroneous oscillatory behaviour and negative probabilities which can occur with both conventional FEM (and finite difference methods). But under more general conditions the main limitation with the FEM is in its applications to higher dimensions where storage problems can pose severe restrictions.

The Path Integral or Cell Mapping method represents a reversion from the fully continuous Markov model described by the FPK equation, back to a Markov model with discrete time or states or both. Table 1 shows that the level of activity using this method is high and the efficiency of 2D solutions compares with FEM predictions for both low-level responses and first-passage statistics. For 3D and higher dimensions however, the method is known to be computationally very expensive [32]. Good reviews of the Path Integral method can be found in references [32] or [34].

Finite difference methods were amongst the earliest used to solve partial differential equations, but they have not been widely applied to the FPK until recently owing to possible problems of numerical instability when attempting to achieve high efficiency. Roberts [5] was one of the early users of an implicit finite difference scheme to obtain first-passage statistics via a 1D FPK equation for an oscillator energy envelope process. More recently, the work of Park and Petrosian [38] deserves mention, since they have examined six finite difference schemes for use with general forms of FPK equation—three fully implicit and three semi-implicit. In the application to the problem of stochastic acceleration in particle physics, they tested a range of performance measures including: numerical stability, accuracy, efficiency, and robustness—concluding that the fully implicit Chang–Cooper algorithm is the most robust–*all* other methods tested in this application suffered from inaccuracy or instability.

The Variational method—eigenfunction expansion replaces the problem of finding the solution of the FPK by an equivalent problem of finding the stationary conditions of a functional. This allows approximate solutions to be obtained via a Rayleigh–Ritz procedure, which according to reference [7] (where a good review can be found) offers a potentially more efficient approach than the FEM, provided that the convergence rate is adequate. The method described in reference [7] uses an eigenfunction expansion of the FPK, in which complex boundary conditions can be incorporated into the functional, allowing use of orthogonal functions in the expansion, which need not satisfy the possibly complex boundary conditions. Testing of the method to predict both the limiting decay rate of the first-passage probability and the mean time to failure, confirmed the accuracy of approximate results given in reference [4] for the linear oscillator. There is however little

known about the convergence of this method for an oscillator with light, but (wholly) non-linear damping, at relatively high normalised barrier heights (i.e. >3).

Very few of the published numerical predictions, obtained by using the methods listed in Table 1, correspond to very small failure probabilities. Indeed none of the methods have been specifically concerned with extreme-value prediction at all, perhaps with the exception of reference [34] where Path Integral predictions for a Duffing oscillator driven by white noise excitation, are focused in the tails of the response amplitude density function. Consequently since little is known about extreme-value prediction, a position has been reached where this survey can be used to justify an appropriate route to efficient reliability assessment for non-linear oscillators. This survey can also be used to identify corresponding numerical FPK methods whose accuracy and efficiency remains to be tested at extreme levels. Essentially, these two points can be combined into the single question which asks whether it makes sense to opt for first-passage failure prediction if it can be shown that very accurate extreme-value probabilities can be obtained via the mean crossing rate using numerical solutions of the stationary FPK equation.

Now, since first-passage statistics can be predicted exactly, for example by using the FEM, it would seem in principle that they offer the most appropriate reliability approach. But while numerical first passage predictions satisfy the requirement for accuracy, there are three reasons why they are very inefficient, proving impractical when probabilities are very small and mean times to failure are long (which is the case of greatest interest in practice [5]). These reasons are as follows.

(1) Solution of a *nonstationary* BK or FPK equation is always necessary—this involves discretization of the time, as well as the space variables, by using for example the FEM/Crank–Nicholson method [26].

(2) The nonstationary FPK/BK solution must be re-obtained in full for *each* (discrete) barrier height.

(3) A very fine mesh is needed to obtain small probabilities if numerical instabilities are to be avoided (as cited in reference [34], for example, in the use of the Petrov–Galerkin FEM).

With points (1) and (2) taken together, if the first-passage failure is needed at a number of discrete barriers (say ten), for a mean failure time of perhaps a thousand response cycles, it is clear that this will require many orders of magnitude more computing time than that needed to obtain a single stationary FPK solution.

Furthermore, in practical situations the initial state is usually unknown and so the need to specify its distribution is an unnecessary complication for long mean failure times since it has very little influence. By contrast, solving only a stationary equation has the advantage that the initial state is not specified at all.

Alternatively approximate first-passage failure could in principle be obtained via the limiting decay given by using an eigenfunction expansion [7] if the (decay rate/crossing rate) criterion justifies it. There are however two possible difficulties here for oscillators with very light non-linear damping. First convergence of the expansion at each of the (discrete) barrier heights may be very slow [7]. And second, since the basis of the limiting decay rate criterion for *finite* barrier heights has never been rigorously justified [7], it could happen that this criterion may be overconservative (as shall be demonstrated in the context of stationary extreme-value prediction in section 5). Furthermore, to obtain the crossing rate accurately, solution of a stationary FPK is required (once only), but if an alternative approach (namely approximate extreme-value prediction) required only this information, it would seem unnecessarily complicated not to use it.

To turn then to a threshold crossing based extreme-value approach, the need will arise in section 5 for an efficient solution of the stationary FPK equation. Since none of the FPK methods in Table 1 have been tested in the role of extreme level prediction, it seems highly appropriate to test the WRM [21–23], and the FEM method [25], since these have been developed primarily for generation of stationary solutions.

3. OSCILLATOR RESPONSE EXTREME-VALUE PREDICTION VIA THE STATIONARY FPK EQUATION

The assumption of an independent up-crossing process allows a stationary response amplitude extreme-value distribution function to be derived in asymptotic form by using only the mean threshold crossing rate. This can be obtained from the joint probability density function of response and its first derivative via a stationary Fokker–Planck equation. Construction of the FPK equation requires only drift and diffusion coefficients, which are obtained directly from the stochastic vibration model when put appropriately into Ito form [13, 19]. A single-degree-of-freedom model is used here, which allows, by appropriate choice of parameters, reduction to two different models needed in the study. This general model is of the form

$$\ddot{Z} + 2\xi\omega_n \dot{Z} + \alpha_1 \dot{Z}Z^2 + \alpha_2 \dot{Z}|\dot{Z}| + \omega_n^2 Z + k_3 Z^3 = Aw(t), \tag{1}$$

which represents an oscillator model with a linear plus two-term non-linear damping, and linear plus cubic stiffness. The excitation $w(t)$ is a unit intensity stationary zero mean Gaussian white noise process, scaled to any required level by parameter A. By setting only the non-linear damping parameters α_1 and α_2 to zero, the first model obtained is a relatively simple Duffing-type oscillator with linear damping. The second model obtained from equation (1), by setting only the linear damping parameter $\xi = 0$, is an oscillator with wholly non-linear damping: i.e., without any linear damping component. This second oscillator is a much more realistic vibration model and is known to describe adequately large amplitude vibration of a clamped–clamped beam, at least up to the tails of the response amplitude marginal probability density function [40].

An explicit stationary FPK solution is available for the simple Duffing model, but there are no exact solutions for the second model. The approximate route chosen here to obtain the extreme-value exceedance probability appropriate for the general model described by equation (1), will now be briefly outlined, first in terms of extreme-value distributions, then in terms of crossing statistics and the Poisson assumption, and finally showing the use of Markov process theory via the Fokker–Planck equation for a SDOF model.

3.1. EXTREME-VALUE EXCEEDANCE PROBABILITIES

In general, the extreme-value $M(T)$ for a stochastic process (or more specifically an oscillator response $Z(t)$) is defined as the maximum value of the process within the time interval $(0, T]$ which can be expressed in mathematical terms [8] as

$$M(T) = \sup\{Z(t) : 0 \leqslant t \leqslant T\}, \tag{2}$$

where, for any sample path, the supremum is in fact the global maximum value in the interval $(0, T]$. The main focus of attention here is on the prediction of the distribution function defined as usual in the form

$$P\{M(T) \leqslant u_T\} = F_M(u_T), \tag{3}$$

where u_T is the threshold level of variable $Z(t)$, or more specifically the extreme exceedance probability, which can be written in terms of the distribution function as

$$P\{M(T) > u_T\} = 1 - F_M(u_T). \tag{4}$$

Now for practical durations appropriate to extreme levels u_T of design interest, $F_M(u_T)$ will be very close to one, and therefore accuracy in the tails of the distribution function (3) is very important. Since in many applications the distribution function has typically been very difficult to obtain, considerable use has been made of the distribution moments such as expected extreme-value. For example, in marine applications, the notional "return period" has been widely used to define the time interval T for which the expected extreme-value is precisely equal to a specified extreme level u_T. While the expected extreme-value is a statistical measure of obvious qualitative value, it is actually not quantitatively useful, as correctly pointed out in reference [41]. This limitation stems from the realisation that the probability of exceeding the expected extreme-value is in fact always relatively high, and cannot therefore be used for meaningful reliability decision making. In this respect the extreme exceedance probability is by contrast a much more useful measure, since a small number is easier to interprete in terms of frequencies of occurrence. Moreover, bandwidth effects have significantly less impact on extreme exceedance probabilities than on expected extreme-values, giving added justification to a decision making approach based on probabilities rather than expected values. These two aspects give further motivation to the objectives of this paper.

3.2. THE POISSON ASSUMPTION OF STATIONARY INDEPENDENT UP-CROSSINGS

For sufficiently high levels u_T, it is shown in reference [8] that the up-crossing intervals tend to become asymptotically independent, which allows the cumulative distribution function (3) to be obtained, since the number of upcrossings per unit time has a Poisson distribution. In accordance with reference [18], this can be written as

$$F_M(u_T) = \exp\{-\upsilon^+(u_T)T\} \quad \text{as } u_T \to \infty, \tag{5}$$

where $\upsilon^+(u_T)$ is the mean threshold crossing rate of level u_T. For stationary vibration responses $Z(t)$, with appropriate sample path properties [8], the mean up-crossing rate can be obtained from Rice's formula [19]

$$\upsilon^+(u_T) = \int_{\dot{z}=0}^{\dot{z}=+\infty} \dot{z} f(u_T, \dot{z})\, \mathrm{d}\dot{z}, \tag{6}$$

where $f(z, \dot{z})$ is the stationary joint probability density function for Z and $\dot{Z}$. This implies that above certain thresholds, for which the Poisson assumption holds, the extreme exceedance probability expressed by equation (4) can be obtained over a finite interval just in terms of the joint properties of response variables Z and $\dot{Z}$.

Naess [1] however suggested that the desired asymptotic convergence is often exceedingly slow, even implying that the asymptotically Poisson character of the up-crossing process may in fact be of rather limited value, especially for narrow-band processes of engineering interest. A correction to the up-crossing rate to account for the effects of bandwidth was therefore proposed by using the concept of "mean joint crossing rate". This involves a zero-memory transformation of an $n(0, 1)$ (standard normal) process to one with the same spectrum and high level crossing rate as $Z(t)$. In the applications in [1], use of this correction does show some noticeable improvement in the accuracy of predictions for a white noise driven linear oscillator with 1% critical damping, but is shown to be less important when damping levels are increased to 4% critical. In another application,

involving non-Gaussian excitation of a linear oscillator, predictions of the expected-extreme, in which bandwidth effects are accounted for, showed error reductions of around 25% for an average of 36 cycles duration, and 10% for 360 cycles—the errors remaining conservative whether bandwidth correction was included or not. These findings correctly apply to predictions of expected extreme-values rather than exceedance probabilities, which, (as pointed-out in reference [41] and mentioned earlier) does not actually offer a very useful reliability measure. The question whether bandwidth is important for exceedance probabilities will therefore be taken up in section 5.

3.3. THE FPK EQUATION FOR THE SDOF OSCILLATOR MODEL

Markov process theory allows the statistical properties of the response trajectories for a class of non-linear oscillator models to be described in terms of the FPK equation [13, 19]. The stationary joint density function needed in equation (6) for use in equations (5) and (4) can therefore be obtained for a stochastic dynamic model of the type given by equation (1) via a 2D FPK equation. It should however again be mentioned at this stage that for non-linear oscillator models in general, correction for the effects of bandwidth cannot be based on the FPK equation alone and therefore one proceeds accepting this limitation only to justify it in section 5. Construction of the FPK associated with equation (1) (and indeed for more general non-autonomous models, with more degrees of freedom) is approached via an appropriate Ito equation [19] of the form

$$\mathrm{d}\underline{z} = \underline{Q}(\underline{z}, t)\,\mathrm{d}t + G(\underline{z}, t)\,\mathrm{d}\underline{b}(t) \tag{7}$$

where in general $\underline{z}(t)$ represents an n-dimensional vector Markov solution process, $Q(\underline{z}, t)$ is an n-dimensional vector of system functions, and $G(\underline{z}, t)\,\mathrm{d}\underline{b}(t)$ is an n-dimensional filtered version of the independent increments of an m-dimensional Wiener process $\underline{b}(t)$ with the properties that

$$E[\underline{b}(t)] = 0 \tag{8}$$

and the increments of the Wiener process satisfy

$$E(\Delta b_i\,(t)\Delta b_j\,(t)) = 2D_{ij}\,\Delta t. \tag{9}$$

Here, the formal derivative of $\underline{b}(t)$ is a unit intensity white noise process $w(t)$, and the matrix $D = \pi I$ (where I is the unit matrix). Equation (1) can be put into the form of equation (7), by using an appropriate state variable description. The general form of the FPK equation for a non-autonomous differential model can be obtained by identifying the drift and diffusion terms [19] to give

$$\frac{\partial}{\partial t} f(\underline{z}, t|z_0, t_0) = \sum_{i=1}^{n}\sum_{j=1}^{n} \frac{\partial^2}{\partial z_i\,\partial z_j}\,[(GDG^{\mathrm{T}})_{ij} f\,] - \sum_{i=1}^{n} \frac{\partial}{\partial z_i}\,(Q_i\,(\underline{z}, t)\,f), \tag{10}$$

where f is the joint transition probability density function $f(\underline{z}, t|z_0, t)$ which is a unique solution of equation (10), subject to a large variety of boundary conditions [13] (appropriately specified shortly for the stationary autonomous case).

When the coefficients in the differential model do not explicitly depend on time, and if the excitation process is independent of the system state, then the Ito equation (7) simplifies to

$$\mathrm{d}\underline{z} = g(\underline{z})\,\mathrm{d}t + G\,\mathrm{d}\underline{b}(t), \tag{11}$$

where $g(\underline{z})$ is a vector of system functions and G is a constant square matrix.

By allowing the initial state to tend infinitely far back into the past, i.e., $t_0 \to -\infty$, then if far field and normalization boundary conditions can be imposed over an unrestricted region Ω in the form

$$f(\underline{z}) \to 0, \quad |\underline{z}| \to \pm\infty, \qquad \text{and} \qquad \int_{\Omega} f(\underline{z})\, \mathrm{d}\underline{z} = 1, \tag{12, 13}$$

then the stationary FPK equation follows,

$$\tfrac{1}{2} \sum_{i=1}^{n} \sum_{j=1}^{n} B_{ij} \frac{\partial^2}{\partial z_i\, \partial z_j} [f(\underline{z})] - \sum_{i=1}^{n} \frac{\partial}{\partial z_i} [g_i(\underline{z})\, f(\underline{z})] = 0 \tag{14}$$

where $B = 2\pi G G^{\mathrm{T}}$ is an $n \times n$ matrix of (white noise) intensities, and $f(\underline{z})$ is the stationary joint probability density function associated with the stationary trajectories of vector process $\underline{z}(t)$.

Specializing this approach to the oscillator model equation (1) gives a two-state vector Markov version of equation (11) described by the Ito equation

$$\begin{bmatrix} \mathrm{d}z_1 \\ \mathrm{d}z_2 \end{bmatrix} = \begin{bmatrix} z_2 \\ -2\xi\omega_n z_2 - \alpha_1 z_2 z_1^2 - \alpha_2 z_2 |z_2| - \omega_n^2 z_1 - k_3 z_1^3 \end{bmatrix} \mathrm{d}t + \begin{bmatrix} 0 & 0 \\ 0 & A \end{bmatrix} \begin{bmatrix} 0 \\ \mathrm{d}b(t) \end{bmatrix}, \tag{15}$$

and the corresponding stationary FPK equation (14) can then be written as

$$\pi A^2 \frac{\partial^2 f}{\partial z_2^2} - \frac{\partial}{\partial z_1} (z_2 f(\underline{z})) + \frac{\partial}{\partial z_2} ((2\xi\omega_n z_2 + \alpha_1 z_2 z_1^2 + \alpha_2 z_2 |z_2| + \omega_n^2 z_1 + k_3 z_1^3) f(\underline{z})) = 0, \tag{16}$$

with the same boundary conditions (12) and (13) as appropriate to a two-state process.

Now if equation (16) can be solved accurately, then use of equations (5) and (6), via the Poisson assumption, allows approximation of the extreme-value exceedance probability via equation (4). The key initial question then for prediction of extreme response statistics appropriate to sample solutions of equation (1), is whether highly efficient solutions of the FPK equation can be obtained to sufficient accuracy in the tails of $f(\underline{z})$, and under what conditions does the Poisson assumption hold. The answer to the first of these questions will now be obtained by using functional-type numerical solutions of the FPK equation.

4. NOMINAL EXTREME EXCEEDANCE PREDICTION BY USING FUNCTIONAL-TYPE NUMERICAL FPK SOLUTIONS

Two of the well-established numerical methods mentioned in section 2 for obtaining stationary solutions of the FPK equation (16) with boundary conditions (12) and (13), are now used to make extreme-value predictions via equations (4)–(6). First, via standard-type weighted residual methods [21–23], by using three suitably chosen types of shape function, and second, a Finite Element method developed by Langley [25], which offers a different form of weighted residual method in the sense that shape functions are defined over finite regions rather than over the entire variate space. Undetermined coefficients, used in both methods, are obtained via a Galerkin-type approach.

The main aim of this section is to establish the accuracy of these methods when used very efficiently in terms of nominal extreme-value predictions for different time intervals of duration T (or corresponding average number of oscillator cycles). For the special case $\alpha_1 = \alpha_2 = 0$ in equation (1), an exact solution of the FPK (given in section 4.4) can be used

via equations (5) and (6) to generate nominally "exact" benchmark extreme-value predictions, but, since in these the Poisson assumption of the independent up-crossings is implicit, they cannot be regarded as definitively accurate in any absolute sense. An absolute comparison by using Monte Carlo simulations is deferred to section 5. But first, brief overviews of the weighted residual and finite element methods are given.

4.1. STATIONARY FPK SOLUTION METHODS BY USING WEIGHTED RESIDUALS

The use of the weighted residual method as applied in references [21–23] can be conveniently described for an n-dimensional FPK and then made specific to the 2D case appropriate to equation (16). It would appear in general that the main advantage of using weighted residuals is their very high efficiency for weakly non-linear systems, especially when using, for example, the WRM developed by Soize [22]. The hope for strongly non-linear oscillator models is that this efficiency is retained. Of particular interest here is the accuracy in the tails of the FPK solution when using different types of base function since this obviously affects the accuracy of extreme-response predictions.

Essentially one assumes in the method that the joint probability density function (jpdf) $f(\underline{z})$ satisfying equation (14) can be approximated in series form,

$$f(\underline{z}) \approx \hat{f}(\underline{z}) = f_s(\underline{z}) + \sum_{i=1}^{N} c_i f_i(\underline{z}), \tag{17}$$

where the function $f_s(\underline{z})$ is chosen to satisfy boundary conditions (12) and (13). Shape functions $f_i(\underline{z})$ are chosen to form a complete basis [20] where coefficients c_i are selected to provide an approximate FPK solution. The usual approach, as adopted here, involves constructing an equation residual for an arbitrary value N in the series approximation, namely

$$R(\hat{f}(\underline{z})) = \tfrac{1}{2} \sum_{i=1}^{N} \sum_{j=1}^{N} B_{ij} \frac{\partial^2}{\partial z_i \, \partial z_j} \hat{f}(\underline{z}) - \sum_{i=1}^{N} \frac{\partial}{\partial z_i} [g_i(\underline{z}) \hat{f}(\underline{z})], \tag{18}$$

where the residual $R(f(\underline{z}))$ gives a measure of how well the trial solution satisfies the FPK equation over the entire domain. If the base functions are chosen correctly, and the coefficients c_i are appropriately adjusted, the residual should rapidly converge to zero everywhere in the region as the number of terms in the series (17) is increased. The weighted residual equation

$$\int_{\Omega} R(\hat{f}(\underline{z})) f_i(\underline{z}) \, \mathrm{d}\underline{z} = 0, \tag{19}$$

plus the normalization condition (13), are used as a basis for obtaining the coefficients c_i, where the weight functions in equation (19) are usually chosen to be the same as the shape functions (Galerkin's method). Equation (19), when combined with the normalization boundary condition, reduces to a system of (generally sparse) linear equations in the unknown coefficients from which a unique set of c_i can be obtained for any particular value of N in equation (17). Previous applications of the WRM to the 2D FPK equation have exploited a double series version of equation (17) in the form

$$f(z_1, z_2) = \sum_{i=1}^{N_1} \sum_{j=1}^{N_2} c_{ij} p_i(z_1) p_j(z_2), \tag{20}$$

which automatically satisfies boundary conditions (12) and (13). And again, on forming the residual in equation (18), unique values of the undetermined coefficients are obtained via equations (13) and (19).

Here one uses two basic types of double-series approximation, first a Gram–Charlier series applied by Bhandari and Sherrer [21], which was also used by Soize [22] in optimum form; and second, a type of pseudo-orthogonal normal density function used by Kunert [23]. This makes a total of three different choices of base function.

The Gram Charlier series functions $P_r(z)$ are defined as

$$p_i(z_1) = \frac{1}{\sqrt{2\pi\sigma_1}} \exp\left(\frac{-z_1^2}{2\sigma_1^2}\right) \mathrm{H}_i\left(\frac{z_1}{\sigma_1}\right), \qquad p_j(z_2) = \frac{1}{\sqrt{2\pi\sigma_2}} \exp\left(\frac{-z_2^2}{2\sigma_2^2}\right) \mathrm{H}_j\left(\frac{z_2}{\sigma_2}\right), \tag{21}$$

where $\mathrm{H}_i(\cdot)$ and $\mathrm{H}_j(\cdot)$ are Hermite polynomials of degree i and j respectively. The orthogonality property of $\mathrm{H}_j(\cdot)$ makes this series very attractive because the integration in the weighted residual equation (19) can be evaluated efficiently in the form

$$\int\int R(z_1, z_2) \mathrm{H}_i\left(\frac{z_1}{\sigma_1}\right) \mathrm{H}_j\left(\frac{z_2}{\sigma_2}\right) \mathrm{d}z_1\, \mathrm{d}z_2 = 0, \tag{22}$$

where equation (22) generates a system of linear equations for the unknown coefficients. The efficiency of the series is known to be quite sensitive [22] to the (standard deviation) parameters σ_1 and σ_2 in equation (21). Bhandari and Sherrer [21], for example, used the standard deviations for the *linear* system (obtained by setting $\alpha_1 = \alpha_2 = k_3 = 0$ in equation (1)); by contrast Soize [22] used optimum standard deviations for the *linearized* system.

The other type of base function tested here [23], is identical to a Gaussian density and used in the form

$$p_i(z_1) = \frac{1}{\sqrt{2\pi\sigma_1}} \exp\left\{-\frac{(z_1 - m_{1_i})^2}{2\sigma_1^2}\right\}, \qquad p_j(z_2) = \frac{1}{\sqrt{2\pi\sigma_2}} \exp\left\{-\frac{(z_2 - m_{2_j})^2}{2\sigma_2^2}\right\}, \tag{23}$$

where the parameters m_{1_i} and m_{2_j} are chosen conveniently to span the entire domain of each variable z_1 and z_2, and where the parameters σ_1 and σ_2 are chosen appropriately small values such that these behave as pseudo-orthogonal base functions leading to sparse coefficient matrices. Use of this method requires truncation of the state space typically up to five equivalent linear standard deviations for both displacement and velocity variables.

Application of Galerkin's method generates a weighted residual,

$$\int\int R(z_1, z_2) \exp\left\{-\frac{(z_1 - m_{1_i})}{2\sigma_1^2}\right\} \exp\left\{-\frac{(z_2 - m_{2_j})}{2\sigma_2^2}\right\} \mathrm{d}z_1\, \mathrm{d}z_2 = 0, \tag{24}$$

and using the normalization condition, results in a particularly simple equation satisfied by the coefficients c_{ij},

$$\int\int f(z_1, z_2)\, \mathrm{d}z_1\, \mathrm{d}z_2 = \sum_{i=1}^{N_1} \sum_{j=1}^{N_2} c_{ij} = 1, \tag{25}$$

allowing c_{ij} to be obtained uniquely from equations (24) and (25). (Note that in the original form [23] stationary solutions were obtained by solving an algebraic eigen problem through discretizing the transient FPK and using inverse iteration to extract the eigenvector associated with the (near) zero eigenvalue. Here one uses the direct method via equation

(24) and the normalization condition, which, for the stationary solution, is mathematically identical).

Extreme exceedance predictions using these three WRM approaches will shortly be compared with both Finite Element and nominally exact FPK based predictions.

4.2. NUMERICAL FPK SOLUTION BY USING THE FINITE ELEMENT METHOD

By approximating the solution to the FPK equation (16) with appropriate shape functions defined over a number of finite regions within the variate space, weighted residuals can be formed which offer a particularly efficient means of obtaining the required solution. Langley [25] developed an FEM specifically for efficient stationary solutions using piece-wise (Lagrange-type) linear shape functions, where the unknown values of the jpdf at a number of nodal points are determined via the "weak" form of weighted residual equation. The same shape functions are also used appropriately for approximating the non-linear functions $g_i(\underline{z})$ within each element. The "weak" form is needed because 1D linear shape functions have only C_0 continuity, whereas the FPK equation (16) includes a second derivative and therefore shape functions need at least C_1 continuity. This limitation was overcome [25] by integrating the residual equation (18), to obtain

$$\tfrac{1}{2}\sum_{i=1}^{n}\sum_{j=1}^{n} B_{ij}\int_R \frac{\partial}{\partial z_i}[w(\underline{z})]\,\frac{\partial}{\partial z_j}[p(\underline{z})] - \sum_{i=1}^{n}\int_R g_i(\underline{z})p(\underline{z})\,\frac{\partial}{\partial z_i}[w(\underline{z})]\,\mathrm{d}\underline{z} = 0, \tag{26}$$

where $g_i(z)$ are drift functions, B_{ij} are the elements in the diffusion matrix in equation (14), and $w(\underline{z})$ is the weight function. The unknown jpdf $p(\underline{z})$ is approximated within rectangular finite elements by

$$p_e(z_1, z_2) = \sum_{i=1}^{4} p_i N_i(z_1, z_2), \tag{27}$$

where p_i is the value of the jpdf at the four nodal corners of each element. The Lagrange-type shape functions $N_i(z_1, z_2)$ are chosen to give unity at corresponding nodes and zero elsewhere. Use of equation (27) in equation (16) allows the integrations in equation (26) to be replaced by a finite sum of integrations over each element. This computationally efficient scheme leads to a system of linear equations for the unknown values of p_i, which can be solved uniquely when the normalization condition is imposed. In implementation in practice one initially assumes a finite region, extending perhaps to four or five standard deviations of the state variables—these are initially estimated by applying statistical linearization to equation (1), and the computational efficiency is further improved by using symmetry.

4.3. NUMERICAL CONSIDERATIONS

Since all four methods described previously can be implemented such that the unknown jpdf reduces to the solution of a sparse system of linear equations, there appears in principle, great scope for obtaining accurate and efficient solutions of 2D FPK equations by using an appropriately large equivalent discrete form. The major practical questions which arise in attempting to exploit sparsity are to do with the space needed to store the coefficient matrix, the achievable machine precision, computer coding considerations, and the computer time needed to generate and solve the resulting sparse system of equations.

In considering use of sparse solution methods there are in fact several possibilities which can initially be explored: first one can attempt to find an accurate FPK solution method (with the smallest number of unknowns) using full storage solution methods—then, if

successful, one can switch to a very efficient (direct) sparse inversion method. A second possibility is to attempt from the outset to use (direct) sparse methods up to their respective storage limitation. And a third possibility is to consider from the outset use of (indirect) iterative methods, perhaps without attempting to store the entire coefficient matrix corresponding to a much larger system of equations than would be possible with direct sparse methods. The attraction of the first option is that an alternative check on the accuracy of the linear equation solution can be made, but the disadvantage is that the solution may be relatively slow but moreover there may be no accurate FPK solution within the full storage space available. The second option goes beyond this full storage limitation but offers no independent check on accuracy, whereas the third option goes further still, but would obviously be slower since repeated generation of part of the coefficient matrix is required and (in general) more time would be needed to solve the system of equations.

Storage requirements of (direct) methods are governed both by the number of non-zero elements and the structure of the coefficient matrix. Although dramatic savings in space are possible, this is not always the case. In fact, in the FEM solution of the FPK equation, the structure of the coefficient matrix is determined by the choice of global node numbering scheme, which, for practical considerations, should ideally be systematic. But a systematic node numbering scheme may lead to a badly structured coefficient matrix with the result that space savings may not be dramatic. This is in contrast to structural FEM where spatial dependence is also not standard so very large problems can often be solved without having to store the assembled coefficient matrix.

For the WRM there is a limitation on the full exploitation of sparsity if high accuracy is required. This follows from at least one precision problem which can arise in the generation of the jpdf when using a series involving a large number of terms, say >40. For example, when using Hermite polynomials in the series expansion (20), the argument of the largest term in each polynomial is raised to the same power as the degree of the polynomial itself. Since in extreme-value predictions these (normalized) arguments are numerically $\gg 1$, an early machine precision limit is expected for high degree polynomials. By contrast the FEM, with rectangular elements, involves at most a weighted sum of just four terms and is therefore not prone to precision errors in the same way. But there is also a practical limitation on the exploitation of sparse storage in the FEM [25] which stems from a computer coding difficulty. This arises in construction of the coefficient matrices, where full storage four-dimensional arrays are needed. Attempts to use four-dimensional arrays in sparse form prove extremely difficult to work with owing to the occasional need for indirect addressing. Although this places a practical storage limitation on the size of the discrete system that can be used, once the coefficient matrix has been constructed, efficient solution can be obtained by fully exploiting a sparse inversion method.

For these reasons—and as reported shortly, owing to the additional computer time needed to generate the coefficient matrices in the WRM compared to the FEM—all the methods tested in this section initially make use of full-storage methods in nominal WRM and FEM based extreme-value predictions and then, where appropriate, use will be made of sparse methods to improve on efficiency.

4.4. A COMPARISON OF NOMINALLY EXACT EXTREME-VALUE PREDICTIONS FOR THE SIMPLE DUFFING OSCILLATOR MODEL

A simple Duffing-type oscillator model is obtained when $\alpha_1 = \alpha_2 = 0$ in equation (1), and for this special case the well-known exact stationary FPK solution [13, 19] of

equation (15) is

$$p(z_1, z_2) = C \exp\left\{\frac{-2\xi\omega_n}{\pi A^2}\left[\frac{z_2^2}{2} + \frac{\omega_n^2 z_1^2}{2} + \frac{k_3 z_1^4}{4}\right]\right\}, \tag{28}$$

where the constant C satisfies the normalization condition. With this solution used in equation (6), the mean up-crossing rate of level u_T, becomes

$$\upsilon^+(u_T) = \frac{\frac{1}{2}\sqrt{\dfrac{A^2}{4\pi\xi\omega_n}}\exp\left[-\dfrac{2\xi\omega_n}{\pi A^2}\displaystyle\int_0^{u_T}(\omega_n^2 z + k_3 z^3)\,\mathrm{d}z\right]}{\displaystyle\int_{-\infty}^{\infty}\exp\left[-\frac{8\xi\omega_n}{A^2}\int_0^{x_1}(\omega_n^2 z + k_3 z^3)\,\mathrm{d}z\right]\mathrm{d}x_1}, \tag{29}$$

and when used in equation (5) gives a benchmark prediction against which both the WRM of section (4.1), and the FEM of section (4.2) can be tested. The Poisson assumption is assumed to hold in all cases; therefore extreme exceedance predictions based on equation (29) are exact in a nominal sense only. The parameter values used in the simple Duffing model are chosen to give extreme-value exceedance probabilities of practical interest in the duration range 25–2500 cycles, corresponding to strongly non-linear responses above three standard deviations of the displacement variable (the linear parameters in the fully linear case conveniently give unit displacement and velocity variances). Table 2 gives the control parameter values used in the comparison and the corresponding standard deviations predicted using the methods.

Although the numerical WRM methods are now used up to a nominal limitation, the exact solution of course has no limitation. For all three WRM applications [21–23] a total of 31 terms was used leading to 961 unknown coefficients, whereas for the FEM, 31 nodal points were used for each state variable giving a total of 961 nodes over one quarter of the doubly symmetrical domain, truncated at $5\sigma_{eq}$ for displacement and velocity variables, representing a region $0 \leqslant z_1 \leqslant 3{\cdot}7$ and $0 \leqslant z_2 \leqslant 5{\cdot}0$ (all four quadrants of this truncated region are used for the WRM application of reference [23]).

Figure 1(a) shows the comparison of the predicted extreme-value exceedance probabilities, over a stationary response duration of $T = 100$ s (corresponding to 25 cycles of undamped free vibration, where the number of cycles $= \omega_{eq} T/2\pi$). The response has been normalized by division with the displacement standard deviation. Figures 1(b) and 1(c) show similar comparisons for $T = 1000$ s (250 cycles) and 10 000 s (2500 cycles) respectively. The probability scale below 10^{-4} has been deliberately truncated on all three figures, whereas the displacement scale extends to 3·8 standard deviations. From these figures the FEM is seen to predict accurately down to 10^{-4} for all three durations. Over the same probability range, only the WRM of Soize [22] compares equally well—the other two WRM approaches [21] and [23] are clearly not efficient, since, to achieve the same level of accuracy, many more terms would be needed, which is undesirable from a precision viewpoint as mentioned earlier and for reasons of computational cost in constructing the coefficient matrices. (Note: in Kunert's method [23] a full, rather than a pseudo-sparse, coefficient matrix has been used; therefore with 31 terms no increase in accuracy could be expected if sparsity were used; moreover, as shown in Table 3, efficiency gains using sparsity would only be achieved when relatively large size coefficients are neglected.)

Beyond the displacement range for which FEM predictions are shown, i.e., below 10^{-4}, both the FEM and WRM exhibit the oscillation phenomenon observed when Gram–Charlier series are used in the method of moment closure, and elsewhere [27]. Since

TABLE 2

Parameter values used in the FPK *based comparison*

FPK solution method	Number of terms in WRM series, or nodes in FEM	Size of variate space domain	Base function control parameters	Predicted response standard deviations	
				σ_z (Theory = 0·5792)	$\sigma_{\dot{z}}$ (Theory = 1·000)
WRM: Bhandari and Sherrer	31 × 31	Infinite	$\sigma_1 = 1{\cdot}0$ $\sigma_2 = 1{\cdot}0$	0·5792	1·000
WRM: Soize	31 × 31	Infinite	$\sigma_1 = 0{\cdot}7407$, $\sigma_2 = 1.0$	0·5792	1·000
WRM: Kunert	31 × 31	$-3{\cdot}7 \leqslant z_1 \leqslant 3{\cdot}7$ $-5{\cdot}0 \leqslant z_2 \leqslant 5{\cdot}0$	$\sigma_1 = 0{\cdot}2467$ $\sigma_2 = 0{\cdot}3333$	0·5792	1·000
FEM: Langley	31 × 31	$0{\cdot}0 \leqslant z_1 \leqslant 3{\cdot}7$ $0{\cdot}0 \leqslant z_2 \leqslant 5{\cdot}0$	–	0·5780	0·999

System parameters $\begin{pmatrix}\text{Simple}\\ \text{Duffing model}\end{pmatrix}$: $\xi = 0{\cdot}5$, $\omega_n = 1{\cdot}0$, $\alpha_1 = 0{\cdot}0$, $\alpha_2 = 0{\cdot}0$, $k_3 = 0{\cdot}5$, $A = 1/\sqrt{\pi}$

Durations (seconds) $T = 100$, 1000, 10 000

TABLE 3

Relative computing times to form coefficient matrices and solve unknowns in the WRM *and* FEM

Method	Number of unknowns in WRM or FEM	Number of non-zeros in coefficient matrix		Time to form coefficient matrix*	Time to solve unknowns* (via full or sparse method)
WRM: Bhandari and Sherrer	31 × 31 = 961	5308	(0·57% full)	746	16 (full)
WRM: Soize	31 × 31 = 961	5308	(0·57% full)	893	16 (full)
WRM: Kunert	31 × 31 = 961	923 521 ($e > 0{\cdot}0$)	(100·0% full)	1162	451 (full)
		230 685 ($e > 10^{-8}$)	(24·0% full)	279	
		192 970 ($e > 10^{-6}$)	(20·8% full)	241	
		154 199 ($e > 10^{-4}$)	(16·6% full)	193	
FEM: Langley	31 × 31 = 961	8274	(0·89% full)	14	60 (full) 7 (sparse)

Time to obtain extreme exceedance probabilities via Monte Carlo simulations (section 5) = 3600–30 000

Note: parameter e in Kunert's method is the absolute magnitude of the smallest element in the coefficient matrix.

* Times shown are CPU seconds on a Solbourne S4000 workstation.

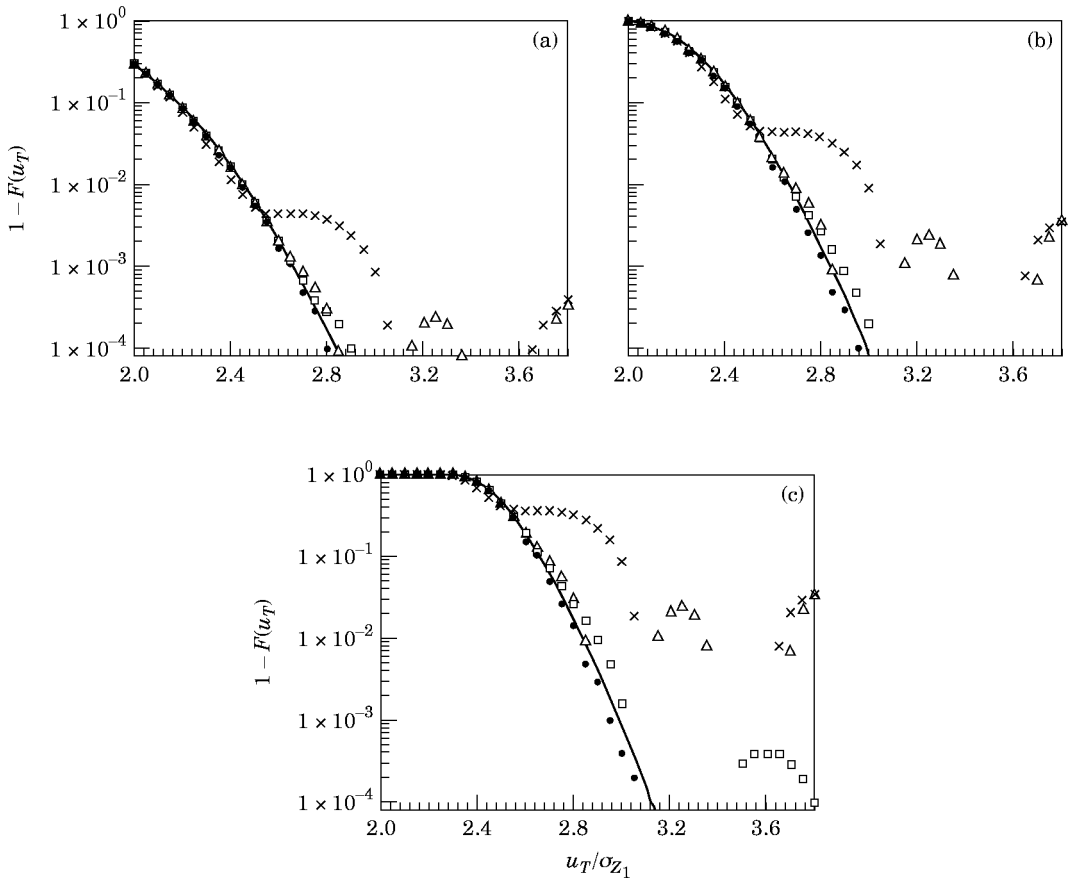

Figure 1. Extreme exceedance probabilities for the simple Duffing model via weighted residual, finite element, and exact FPK solutions: (a) $T = 100$ s (25 cycles); (b) $T = 1000$ s (250 cycles); (c) $T = 10\,000$ s (2500 cycles). ——, "Exact"; ×, Bhandari and Sherrer; □, Soize; △, Kunert; ●, Langley, $31 \times 31 = 961$ nodes.

this phenomenon gives negative probability predictions it is obviously impossible to show fully this effect on a logarithmic scale. Predictions by using the FEM remain accurate down to 10^{-4} but then suddenly plunge to negative values becoming positive only at relatively large displacement. By contrast predictions for all three WRM techniques show oscillations in a much more obvious way giving false (positive) probabilities between three and four standard deviations as shown in Figures 1(a)–1(c). The potential for misinterpreting predictions in this region is therefore much higher with the WRM than the FEM.

From an efficiency viewpoint, the computational efforts needed for marginal probability density prediction by using the FEM and the WRM [21] have been compared in reference [25] showing that the FEM is much faster for oscillators with reasonably strong non-linearity. In making the same comparison for extreme-value prediction, one focuses on two aspects of the computational requirements, namely (i) space requirements and (ii) computation times involved in constructing the coefficient matrix and subsequently in solving the system of linear equations. Owing to the computational time needed to construct the coefficient matrices with the WRM (shown in Table 3), only the FEM has been extended to examine the benefits of using sparse technology. The space requirement (using NAG library sparse routines F04AXF/F01BRF) depends on the scaling and structure of the coefficient matrix. If the structure is poor, then there will be considerable

growth (fill-in) during the direct solution factorisation process. For the FEM, there is in fact quite considerable growth during fill-in, such that if the computer coding difficulties mentioned in section 4.3 can be overcome only a two or threefold increase in the number of elements can be expected for each dimension of a 2D mesh above the full storage limit. The obvious way to improve this is to use a better node numbering scheme but this proved unnecessary, both for this problem and in the problem examined in section 5, because an efficient method was found needing less than the space available.

Turning now to the question of computational cost, for comparison Table 3 shows the relative computing times involved (absolute figures are not very meaningful). For extreme response prediction, the efficiency gain of the FEM compared with the WRM is clearly maintained typically giving around a 40-fold overall speed advantage.

When the accuracy and computational efficiency are taken collectively into account, the Finite element of [25] is superior to the WRM of Soize [22]—whereas the other two WRM methods are totally unsuitable for efficient extreme-value prediction.

The Poisson assumption of independent up-crossings has so far been taken to hold in all these predictions; therefore this now needs to be checked by using lightly damped non-linear oscillator models, before the FEM can be regarded as an genuinely accurate approach to extreme-value prediction.

5. A COMPARISON OF FEM BASED PREDICTIONS WITH MONTE CARLO SIMULATIONS

The importance of the Poisson assumption will now be examined by using two oscillators both derived from equation (1): a simple Duffing oscillator, the same as previously used, and second, a more representative non-linear random vibration model which has been shown experimentally to model adequately large amplitude single co-ordinate responses of a clamped–clamped beam [40]—this model has wholly non-linear damping. The choice of damping parameter, used in the simple model, is however made so that for the response amplitudes of interest, the damping levels of the two systems are statistically equivalent. The parameters chosen in this model are not arbitrary since they have been obtained by using parameter estimation techniques applied to real data obtained from an experimental test rig incorporating a clamped–clamped steel beam of 1 m length and section 25 mm by 3 mm [40]. A clamped beam element actually forms an important structural member in its own right, used for example in bracing members in offshore structures and narrow stretched panels in aircraft [42]. But this particular rig was developed to examine the use of extreme-value techniques on a real structure: i.e., one which would allow sufficient data to be generated for model verification in a controlled series of experiments by using a sufficiently "simple" non-linear system in which additional effects such as the temperature variations in reference [42] are excluded. Satisfying all of these requirements simultaneously can often prove very difficult. The test beam was forced to vibrate randomly in air by using a white noise driven shaker positioned at one end of the beam with various measurements of excitation force and displacement appropriately taken to enable parameter assignment via parameter estimation methods [40]. The particular damping model has been constructed by using a combination of models proposed for vibrating beams which include the combined effect of fluid–structure interaction, structural radiation effects and material damping [40]. Predictions will shortly be shown of extreme exceedances obtained by using the FEM on these two models compared with those given by Monte Carlo simulations. The conventional time-domain simulation method used here is first described briefly.

5.1. CONVENTIONAL MONTE CARLO SIMULATION TECHNIQUE

Monte Carlo simulations offer the most flexible way of examining strongly non-linear stochastic dynamic behaviour except for extreme-value analysis at realistic probability levels, where the method is usually computationally prohibitive [16]. Conventional time-domain simulation involves three stages: (1) a pre-processing stage, where a representative number of excitation sample paths with statistical properties appropriate to the model of equation (1) are constructed; (2) an numerical integration stage (here a standard fourth order Runge–Kutta scheme is used); and (3), a post-processing stage, which involves two activities, the first involving transient removal from a number of output sample paths, each of length T, and the second in which global maxima for each section are identified for use in estimation of the extreme exceedance probability. In stage (2), a truncated Whitaker filter [43] is used to allow convergence of the numerical integration, because white noise samples of the excitation process are assembled at discrete time intervals of duration Δt, giving a uniformly increasing Nyquist bandwidth $f_n = 1/2\Delta t$ as $\Delta t \to 0$. This has the effect of creating noisier excitation samples as $\Delta t \to 0$. By fixing Δt, however, use of the Whitaker filter allows interpolation to smaller time steps $\Delta\tau$, thus generating rapid reduction of the truncation error. Accurate Monte Carlo simulation of the extreme-values requires Δt to be suitably chosen to give a Nyquist bandwidth many times the characteristic bandwidth of the system, with $\Delta\tau$ selected somewhat smaller to meet the numerical convergence requirements. The importance of selecting the correct value for $\Delta\tau$ will be demonstrated shortly. The parameter values used in the simple Duffing model are as follows: $\xi = 0{\cdot}0138$, $\alpha_1 = 0{\cdot}0$, $\alpha_2 = 0{\cdot}0$, $\omega_n = 144{\cdot}34$, $k_3 = 3021$, $A = 200$; correspondingly for the beam model the values are $\xi = 0{\cdot}0$, $\alpha_1 = 0{\cdot}812$, $\alpha_2 = 0{\cdot}015$, $\omega_n = 144{\cdot}34$, $k_3 = 3021$, $A = 200$. Application of statistical linearization to the beam model gives $\xi_{eq} = 0{\cdot}0138$, identical in damping level to the simple model. Simulations reveal respective bandwidth parameter values $\varepsilon = 0{\cdot}96$ for the Duffing model, and $\varepsilon = 0{\cdot}97$ for the beam model. The bandwidth parameter estimate shown here for the simulated data was obtained by using an estimate based on the ratio $\varepsilon =$ (number of zero upcrossings/number of local maxima). For long run simulations of an ergodic process this approaches the estimate $\varepsilon = \sigma_{\dot z}^2 / \sigma_z \sigma_{\ddot z}$. Since the bandwidth of the simulated excitation data (in filtered form) is not infinite, estimates of ε are indeed meaningful. This is in contrast to theoretical Markov trajectories as obtained from the FPK equation, where this definition of bandwidth will always be zero regardless of the damping level. Figure 2 shows power spectral estimates obtained from simulated samples of the excitation and response processes for both oscillator models, clearly demonstrating that responses are very narrow-band. These spectra have been conveniently scaled to allow comparison with the excitation in the frequency domain, where it can be seen that there is no noticeable effect of the use of different damping models. The implications of this insensitivity on frequency domain estimation of nonlinear oscillator damping parameters has been discussed fully in reference [44].

Figure 3(a) shows the comparison of extreme-value exceedance probabilities for the simple Duffing model obtained via Monte Carlo simulation and 961 node FEM–FPK predictions corresponding to a duration of $T = 1$ second (nominally "exact" solutions are also shown). Symmetry allows a quarter region to be used for generating the FEM solution: i.e., from 0 to 5 standard deviations. Different simulation results are shown for three respective time steps $\Delta\tau = 0{\cdot}004$, $0{\cdot}002$, and $0{\cdot}001$ s, used in the Whitaker filter, where the large time step is fixed at $\Delta\tau = 0{\cdot}004$ (interpolation therefore being used in two cases). Figures 3(b) and 3(c) show similar comparisons for $T = 10$ and 100 s, respectively. These FEM predictions have been obtained after initially studying convergence by using an

increasing number of nodes. This information is not shown since one can also compare with the "exact" solution—showing there is no doubt about the adequacy of 961 node predictions. By contrast for the beam model (for which nominally "exact" predictions are not possible) Figure 4 (for each duration) shows convergence of the FEM predictions as the number of nodes is increased from 441 through to 2601 nodes. Figures 5(a)–(c) show a corresponding set of results for the beam model for each duration separately in which simulations are included with both 961 and 2601 node FEM predictions. These show that for practical purposes, 961 node FEM predictions are also adequate for the beam model. To achieve low statistical variability in the Monte Carlo simulations a large number of extreme values are needed for highly confident probability estimates. The size of the sample size needed can be estimated in advance because the statistical variability in an extreme exceedance estimate $\hat{p}$ can be predicted by using the ratio $\sigma_{\hat{p}}/\hat{p} = 1/\sqrt{N_p}$, where $\sigma_{\hat{p}}$ is the standard deviation in $\hat{p}$ and N is the sample size. Clearly, for low probabilities, a large value of N is needed which is very computionally demanding for large durations. Here a value $N = 1000$ extreme-values was used for each duration, giving reasonably confident estimates of p above 10^{-2}. Below this probability level, less confidence can be attached to the simulation results. The simulation time needed here (using a Solbourne S4000) varied from 1 CPU h for $T = 1$; to 8 CPU h for $T = 100$. By contrast the 961 node FEM predictions are again extremely fast (see Table 3 for the Duffing model times) needing only 27 CPU s total—giving a speed advantage over simulation of between 100 and 1000 times, depending on the duration. The 2601 node FEM predictions are somewhat slower needing 255 CPU s, but still giving between 15 and 100 fold speed advantage.

5.2. DISCUSSION OF RESULTS

Two important results are revealed in Figures 3(a)–(c), corresponding to the simple Duffing model. First, on the question of convergence of the numerical integration scheme when using the Whitaker filter, it is clear that the best choice of interpolation time step has been identified, namely $\Delta\tau = 0{\cdot}001$. In fact, any small reduction in the large time step from $\Delta t = 0{\cdot}004$ only produces less efficient simulations, without any increase in accuracy. Conclusions hereafter will therefore be based on the converged simulation results: i.e.,

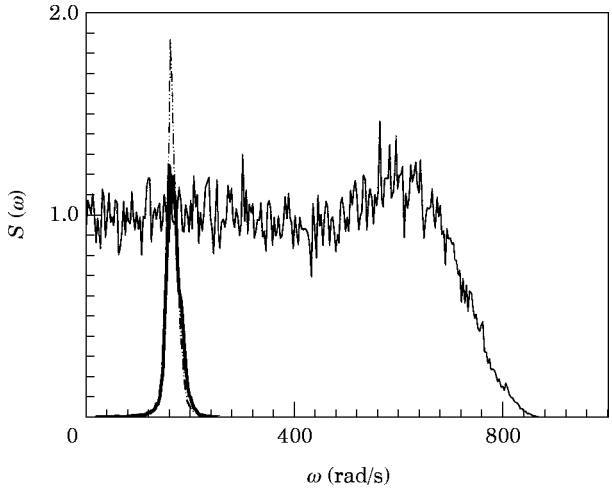

Figure 2. Excitation and response spectra via Monte Carlo simulation. ——, Excitation; ——, simple Duffing oscillator (linear damping) (scaled by factor of 8); –· ·–· ·–, beam model with non-linear damping (scaled by factor of 8).

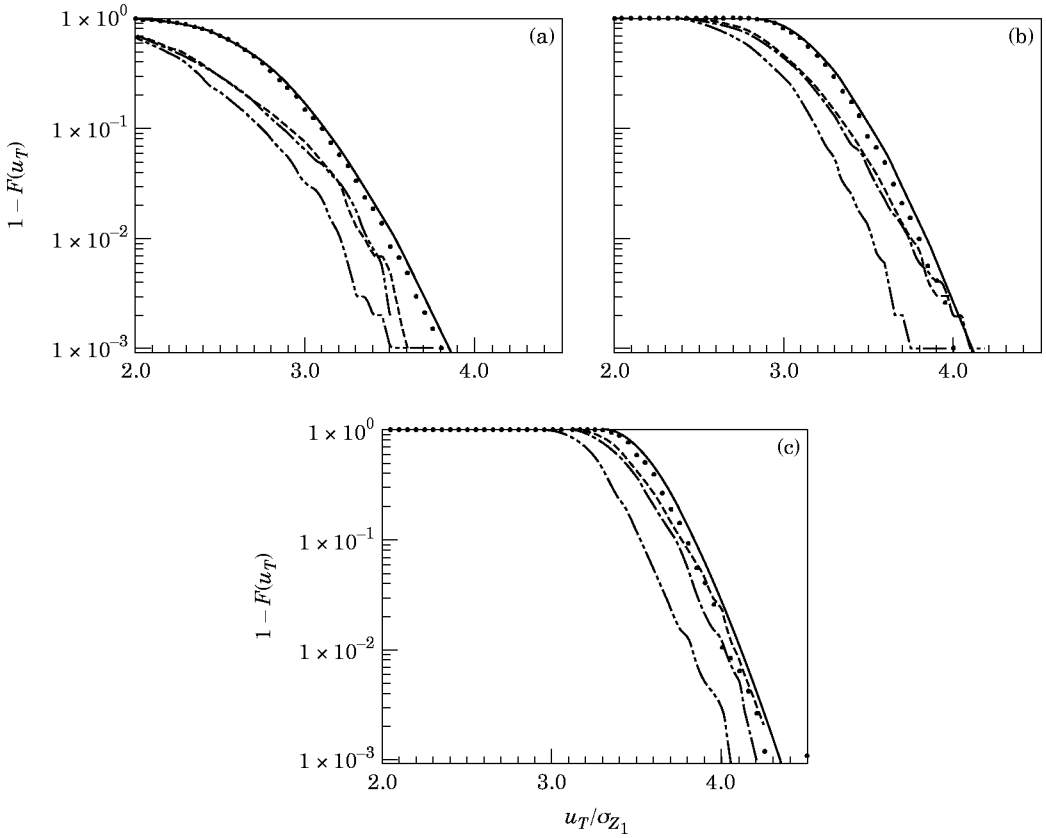

Figure 3. Extreme exceedance probabilities for the simple Duffing model via finite element FPK solutions and Monte Carlo simulation: (a) $T = 1$ s (27·5 cycles); (b) $T = 10$ s (275 cycles); (c) $T = 100$ s (2750 cycles). ——, "Exact"; –·· ·–·· · , simulated response ($\Delta\tau = 0{\cdot}004$ s); –·–·– , simulated response ($\Delta\tau = 0{\cdot}002$ s); -------, simulated response ($\Delta\tau = 0{\cdot}001$ s); ●, finite element (Langley), $31 \times 31 = 961$ nodes.

$\Delta\tau = 0{\cdot}001$. The second important result concerns the Poisson assumption, since Figures 5(a)–(c) clearly demonstrate that, for a short duration $T = 1$ s (27·5 cycles) in the case of the simple Duffing model with linear damping of 1%, threshold up-crossings are clearly not independent for probability levels above 10^{-3}. By contrast predictions for $T = 100$ (2750 cycles) show very good agreement between simulations, demonstrating that the FEM–FPK approach is acceptable below 10^{-1}.

For the non-linearly damped beam model, the level of agreement in the FEM predictions shown in Figures 5(a)–(c) clearly demonstrates that the Poisson assumption seems to hold for all three durations (i.e., $T = 1, 10, 100$ s) below a probability level of 10^{-1}. Again the use of the Whitaker filter for all the results would suggest an appropriate interpolation step has been used. (Note that the simulation result for Figure 5(b), i.e., $T = 10$ s, at the pre-converged value $\Delta\tau = 0{\cdot}002$, shows the kind of statistical variability which can occasionally occur in direct estimates of the extreme exceedance probability when using conventional Monte Carlo simulation—this is why use of theoretical methods such as those based on the FPK equation are attractive.) Overall these results show that for a realistic non-linearly damped oscillator model, with a damping level of 1% or greater, accurate extreme exceedance prediction can indeed be made via the stationary FPK equation without need to account for bandwidth.

It was mentioned in the Introduction (and section 2) that the "limiting decay rate of the first-passage probability" has been used as a criterion for determining the barrier height above which first-passage intervals can been assumed to be independent [2–7]. The main reason why the Poisson assumption does not hold, below certain levels, is usually given as being due to the effect of clustering (or "clumping"; e.g., see references [1], [4] or [6]). Clustering therefore occurs only at high levels for which the Poisson assumption still does not hold. Conversely, for example, stationary normal sequences do not exhibit clustering at the high levels required for the Poisson assumption to hold, regardless of the level of correlation [45]. Since it is reported that measured first-passage times for narrow band processes are considerably longer than predicted when assuming independent first-passage intervals, it is of interest to establish whether the limiting decay rate criterion can be of use in stationary extreme-value prediction. To answer this question Figures 3(a)–(c) and Figures 5(a)–(c) are used to identify the (normalized) levels above which stationary extreme-values are independent. These are positioned between 3·9 and 4·2 for the simple Duffing model, and between 2·9 and 3·2 for the beam model, and for convenience these regions are labelled ① and ② respectively. Figure 6 shows the first-passage (limiting decay rate/crossing rate) ratio α/υ for a Duffing model [4], which is actually taken from Figure 9 of reference [4] corresponding to a "B" type barrier, on which the present regions ① and ② are superposed. The parameter ε^2 taken from reference [4] and again used in Figure 6 corresponds to non-linearity in stiffness, and the parameter $\mu\zeta$ gives the linear damping level (where μ is very close to 1). The non-linear stiffness value for both our Duffing and beam models translates here into the value $\varepsilon^2 = 0{\cdot}14$ and the damping level (or corresponding equivalent damping) as given in section 5.1 is just over 1%. The Duffing model here therefore falls tightly within the lower set of curves in Figure 6 (the upper set corresponds to around 8% damping). Region ② for the beam model, with non-linear damping can be justifiably shown on the same figure since the overall damping level is important here [4]. Now, when the ratio $\alpha/\upsilon = 1$, the criterion gives the appropriate first-

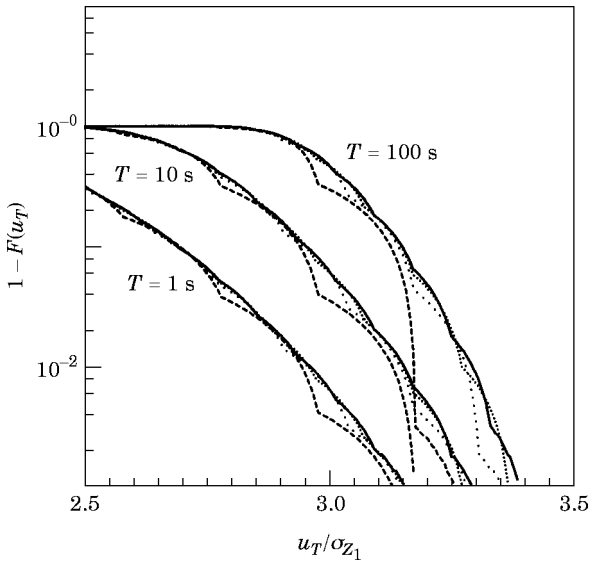

Figure 4. Extreme exceedance probabilities for the beam model, showing converging finite element FPK solutions obtained by using an increasing number of elements for different durations: $T = 1$ s (27·5 cycles); $T = 10$ s (275 cycles); $T = 100$ s (2750 cycles). ----------, $21 \times 21 = 441$ nodes; · · · · · · · · · · , $31 \times 31 = 961$ nodes; ....., $41 \times 41 = 1681$ nodes; ———, $51 \times 51 = 2601$ nodes.

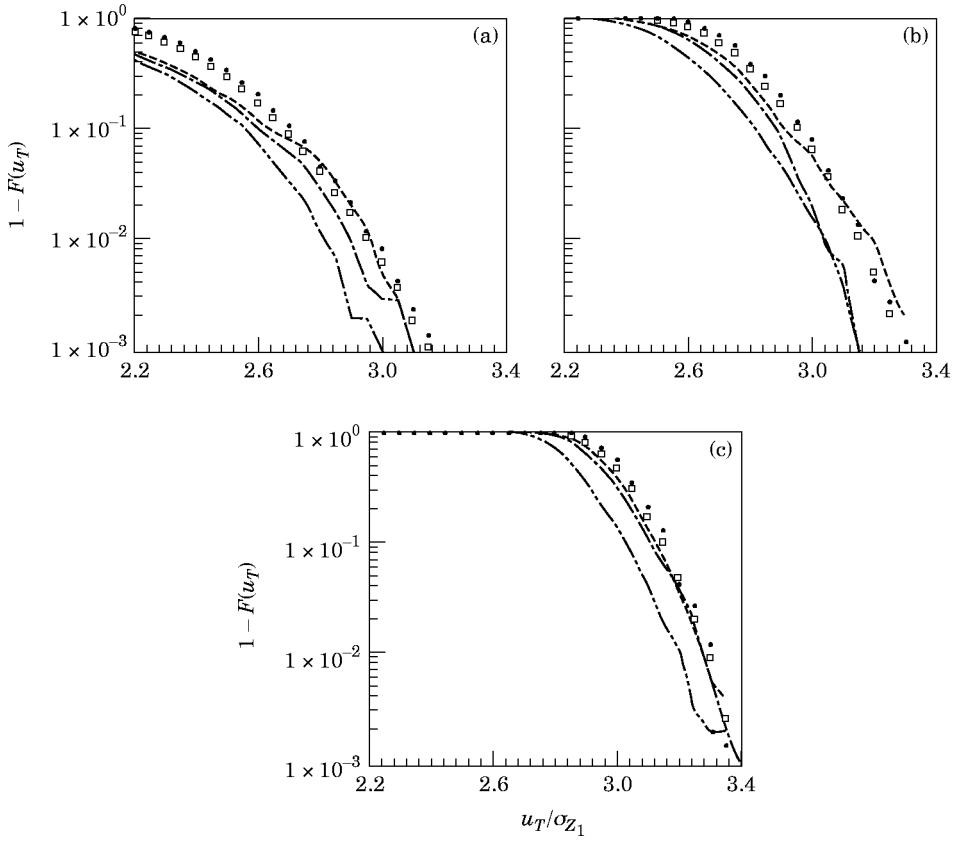

Figure 5. Extreme exceedance probabilities for the beam model with non-linear damping via finite element FPK solutions and Monte Carlo simulation: (a) $T = 1$ s (27·5 cycles); (b) $T = 10$ s (275 cycles); (c) $T = 100$ s (2750 cycles). $-\cdot\cdot-$, simulated response ($\Delta\tau = 0{\cdot}004$ s); $-\cdot-\cdot-$, simulated response ($\Delta\tau = 0{\cdot}002$ s); -------, simulated response ($\Delta\tau = 0{\cdot}001$ s); ●, FEM, $31 \times 31 = 961$ nodes; □, FEM, $51 \times 51 = 2601$ nodes.

passage barrier height above which the Poisson assumption can be assumed to hold. Clearly for 1% damping, superposition of the stationary extreme-value results shown by ① and ② demonstrates that the Poisson assumption actually holds at very much lower levels. Since the accuracy of the linear part of this decay rate information has been confirmed by Langley [7], and since the accuracy of the simulations used to confirm the decay rate criterion by Crandall [2] has already been improved by Roberts [3], and since the present simulation method has been confirmed elsewhere, there is little reason to doubt the quality of the information shown on Figure 6. The only remaining reason for this difference is that, for light damping, the transient part of the limiting decay rate becomes insignificant only when the barrier height is large (and therefore when the mean first-passage interval $\bar{T}$ is large, thereby rendering the transient time a relatively small fraction of the total first passage time). Consequently for α/υ to be of practical value for lightly damped stationary processes, the transient part of the limiting decay rate needs to be removed. However the difficulty here is that the transient part is theoretically infinite and so the practical amount to be removed is rather arbitrary. This suggests that the limiting decay rate of the first-passage probability is in fact grossly overconservative for stationary extreme-value prediction.

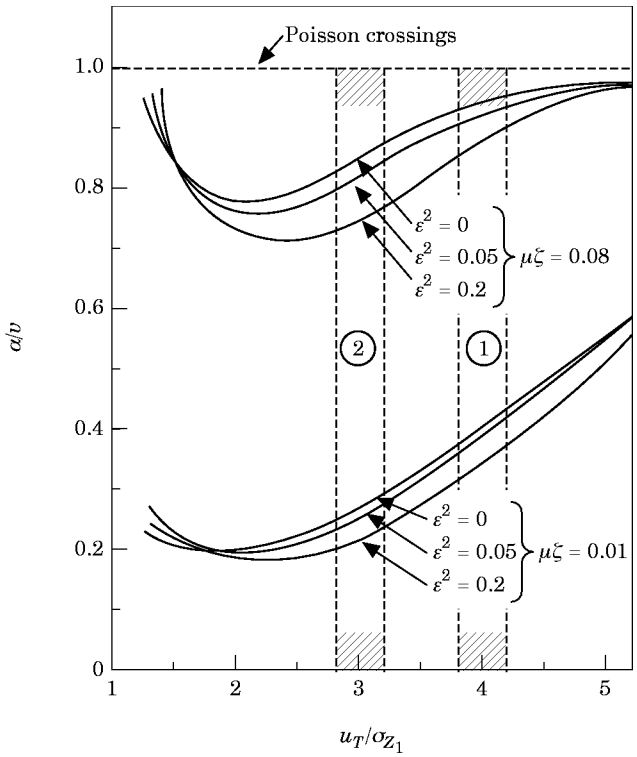

Figure 6. Variation in the normalized limiting decay rate of the first-passage probability for a Duffing-type model with a "B" type barrier (from reference [4]) showing regions ① and ② superposed, corresponding to regions of the stationary extreme exceedance thresholds above which the Poisson assumption holds. Region ①: Duffing model with 1.38% critical damping; region ②: non-linearly damped beam model with 1·38% equivalent linear damping.

A further point of note derived from the extreme-value predictions in Figures 3 and 5 as shown on Figure 6, is that dependence existing at certain levels for the Duffing model seems to have been eliminated at corresponding levels for the non-linearly damped model—as indicated by the difference between region ① and ②. Therefore by implication one demonstrates that, for stationary extreme-values, non-linearity in damping (in addition to the degree of damping in the system [4]), provides a mechanism for relieving the effect of clumping in the peaks of a highly correlated process. The effect of non-linearity in damping can therefore be interpreted qualitatively as a form of strong "mixing" [45], which has the effect of lowering the threshold for which the Poisson assumption holds.

Finally, the authors mention in passing that Langley's finite element method [25] has been extended in reference [40] to response prediction for a coupled system of non-linear stochastic oscillators previously studied in reference [21]. But whilst predictions of reasonably accurate low order response moments are possible by using this method, it is apparent for generation of marginally accurate extreme response statistics that substantial computer memory is needed (possibly around 10^4 Mbytes). Although this sort of working space is not currently available to users, eventually it may become routine, opening up the possibility of using the FPK equation as an alternative to simulation for extreme-value analysis of MDOF systems.

6. CONCLUDING REMARKS

The accuracy of two different functional-type numerical methods for solving the FPK equation has been demonstrated for the purpose of predicting extreme exceedance probabilities associated with white noise driven non-linear oscillators. These methods were initially tested to find out which converges first, and therefore, which is most efficient. The importance of the effect of bandwidth on wholly FPK based extreme-value predictions, via the FEM, has been tested by comparison with Monte Carlo simulations. This was designed to expose any departure from the Poisson assumption of independent up-crossings on stationary response sample paths, at threshold levels and durations of practical interest. Two non-linear oscillator models were examined both around the same 1% overall damping level: one with wholly linear damping; the other with wholly non-linear damping.

The study demonstrates that highly efficient finite element (FEM) based extreme-value predictions are substantially more accurate than the Weighted Residual method (WRM). Moreover, in exploiting FEM based extreme-value predictions, for two different oscillator models, comparison with conventional Monte Carlo simulations shows that, for the particular oscillators studied, bandwidth is important only for the linearly damped model over short durations. For the model with wholly non-linear damping, bandwidth is found not to be important for any durations and probability levels considered. It is also demonstrated that the limiting decay rate of the first-passage probability, which is useful as a criterion for establishing the first-passage barrier height above which the Poisson assumption holds, proves grossly overconservative as a corresponding criterion for use in stationary extreme-value prediction. Finally, since the non-linear damping model used here is appropriate for random vibration of a clamped-clamped beam, the conclusion of the study is that, if equation (1) holds with the particular parameter set chosen, extreme exceedance probabilities of practical interest can be obtained accurately by using a prediction method based wholly on the stationary Fokker–Planck equation.

REFERENCES

1. A. Naess 1990 *Journal of Sound and Vibration* **138**, 365–380. Approximate first-passage and extremes of narrow-band Gaussian and Non-Gaussian random vibration.
2. S. H. Crandall, K. L. Chandiramini and R. G. Cook 1966 *Journal of Applied Mechanics* **33**, 532–538. Some first-passage problems in random vibration.
3. J. B. Roberts 1974 *American Institute of Aeronautics and Astronautics Journal* **12**, 1636–1643. Probability of first passage failure for stationary random vibration.
4. J. B. Roberts 1978 *Journal of Sound and Vibration* **56**, 71–86. First passage time for oscillators with non-linear restoring forces.
5. J. B. Roberts 1986 *Journal of Sound and Vibration* **109**, 33–50. First passage time for randomly excited non-linear oscillators.
6. R. S. Langley 1988 *Journal of Sound and Vibration* **122**, 261–275. A first passage approximation for normal stationary random processes.
7. R. S. Langley 1988 *Journal of Sound and Vibration* **123**, 213–217. A variational formulation of the FPK equation with application to the first passage problem in random vibration.
8. M. R. Leadbetter, G. Lindgren and H. Rootzén 1983 *Extremes and Related Properties of Random Sequences and Processes*. New York: Springer-Verlag.
9. A. M. Hasofer and P. Petocz 1984 in *Statistical Extremes and Applications* (editor J. Tiago de Oliveira); New York: D. Reidel, 503–512. Extreme response of a linear oscillator with modulated random excitation.
10. M. R. Leadbetter and H. Rootzén 1988 *Annals of Probability* **16**, 431–478. Extremal theory for stochastic processes.
11. A. M. Hasofer 1996 in *Mathematical Models for Structural Reliability Analysis* (editors F.

Casciati and J. B. Roberts); CRC Press Mathematical Modelling Series; Chapter 4, 195–226. Non-parametric estimation of failure probabilities.
12. J. B. Roberts and P. D. Spanos 1990 *Random Vibration and Statistical Linearization*. Chichester: John Wiley.
13. Y. K. Lin and G. Q. Cai 1995 *Probabilistic Structural Dynamics*. New York: Mc-Graw-Hill.
14. S. R. Winterstein and O. B. Ness 1989 in *Computational Mechanics of Probabilistic and Reliability Analysis*; Lausanne: Elme Press, Chapter 21, 452–478. Hermite moment analysis of non-linear random vibration.
15. A. Naess, F. Galeazzi and M. Dogliani 1992 *Applied Ocean Research* **14**, 71–81. Extreme Response predictions of non-linear compliant offshore structures by stochastic linearization.
16. S. R. Winterstein and R. Torhaug 1993 *Proceedings of the* 12*th International Conference of the OMAE-ASME* **2**, 251–258. Extreme response of jack-up structures from limited time-domain simulation.
17. J. F. Dunne 1996 *Journal of Sound and Vibration* **193**, 597–629. An optimal control approach to extreme local maxima for stochastic Duffing-type oscillators.
18. A. Naess 1984 *Applied Ocean Research* **6**, 173–174. Technical note: on a rational approach to extreme value analysis.
19. T. T. Soong 1973 *Random Differential Equations in Science and Engineering*. New York: Academic Press.
20. C. Soize 1994 *The Fokker–Planck Equation for Stochastic Dynamical Systems and its Explicit Steady State Solutions*. Singapore: World Scientific.
21. R. G. Bhandari and R. E. Sherrer 1968 *Journal of Mechanical Engineering Science* **10**, 168–174. Random vibration in discrete non-linear dynamic systems.
22. C. Soize 1989 *Probabilistic Engineering Mechanics* **3**, 196–206. Steady state solution of Fokker–Planck equation for higher dimensions.
23. A. Kunert 1991 *Vibration Analysis—Analytical and Computational* ASME DE-37, 57–60. Efficient numerical solution of multidimensional Fokker–Planck equations associated with chaotic and non-linear random vibrations.
24. L. A. Bergman and J. C. Heinrich 1981 *Earthquake Engineering and Structural Dynamics* **9**, 197–204. On the moments of time to first passage of the linear oscillator.
25. R. S. Langley 1985 *Journal of Sound and Vibration* **101**, 41–54. A finite element method for the statistics of non-linear random vibration.
26. B. F. Spencer Jr and L. A. Bergman 1993 *Non-linear Dynamics* **4**, 357–372. On the numerical solution of the Fokker–Planck equation for non-linear stochastic dynamics.
27. H. T. Banks, H. T. Tran and D. E. Woodward 1993 *SIAM Journal of Numerical Analysis* **30**, 1574–1602. Estimation of variable coefficients in the Fokker–Planck equations using moving node finite elements.
28. H. U. Köylüoğlu, S. R. K. Nielsen and R. Iwankiewicz 1994 *Journal of Sound and Vibration* **176**, 19–33. Reliability of non-linear oscillators subject to Poisson driven impulses.
29. M. A. Elgebeily and H. E. E. Shabaik 1994 *Communications in Numerical Methods in Engineering* **10**, 763–771. Approximate solution of the Fokker–Planck–Kolmogorov equation by finite-elements.
30. T. Kapitaniak 1985 *Journal of Sound and Vibration* **102**, 440–441. Stochastic response with bifurcations to non-linear Duffing's oscillator.
31. J.-Q. Sun and C. S. Hsu 1988 *Journal of Sound and Vibration* **124**, 233–248. First-passage time probability of non-linear stochastic systems by generalised cell mapping.
32. A. Naess and J. M. Johnsen 1991 in *Computational Stochastic Methods* (editors P. D. Spanos and C. A. Brebbia) co-published: Computational Mechanics Publications; Southampton—Elsevier Applied Science; London, 279–291. The path integral solution applied to the random vibration of hysteretic systems.
33. A. N. Drozdov 1992 *Physics Letters A* **171**, 175–182. Path integral solution of the Fokker–Planck equation via a generalized Trotter formula.
34. H. U. Köylüoğlu, S. R. K. Nielsen and A. C. Cakmak 1995 *Structural Safety* **17**, 151–165. Fast cell-to-cell mapping (path integration) for non-linear white noise and Poisson driven impulses.
35. R. Iwankiewicz and S. R. K. Nielsen 1996 *Journal of Sound and Vibration* **195**, 175–193. Dynamic response of non-linear systems to renewal impulses by path integration.
36. J. S. Mckenzie, M. R. O'Brian and M. Cox 1991 *Computer Physics Communications* **66**, 194–206. Solution of 3-dimensional Fokker–Planck equations for Tokamak plasmas using operator splitting technique.

37. E. M. Epperlein 1994 *Journal of Computational Physics* **112**, 291–297. Implicit and conservative difference scheme for the Fokker–Planck equation.
38. B. T. Park and V. Petrosian 1996 *The Astrophysical Journal Supplement Series* **103**, 255–267. Fokker–Planck equations of stochastic acceleration: a study of numerical methods.
39. W. V. Wedig 1996 in *Advances in Non-linear Stochastic Mechanics*: Kluwer Academic, 469–478. Stability and invariant measures of perturbed dynamical systems.
40. M. Ghanbari 1996 *D. Phil. Dissertation*, *University of Sussex*. Extreme response prediction for random vibration of a clamped-clamped beam.
41. S. McWilliam and R. S. Langley 1993 *Applied Ocean Research* **15**, 169–181. Extreme values of first- and second-order wave induced vessel motions.
42. R. R. Chen, C. C. Mei and H. F. Wolfe 1996 *Journal of Sound and Vibration* **195**, 719–738. Comparison of finite element non-linear beam random response with experimental results.
43. B. W. Oppenheim and P. A. Wilson 1980 *Journal of Ship Research* **24**, 181–189. Continuous digital simulation of the second order slowly varying drift force.
44. J. B. Roberts, J. F. Dunne and A. Debonos 1995 *Probabilistic Engineering Mechanics* **10**, 199–207. A spectral method for estimation of non-linear system parameters from measured response.
45. M. R. Leadbetter 1995 *Journal of Statistical Planning and Inference* **45**, 247–260. On high level exceedance modeling and tail inference.